Modeling High-Viscosity, Melt-Phase, Condensation Polymer Reactors with a Time-Scales Analysis

KENDREE J. SAMPSON* and SWATI NEOGI

Department of Chemical Engineering, Ohio University, Athens, Ohio 45701

SYNOPSIS

Mathematical models for simultaneous reaction and mass transfer occurring in the manufacture of high-viscosity, condensation polymers are considered. The specific example of polycondensation of polyethylene terephthalate is examined. Reactor performance is estimated by using a kinetic expression modified by an effectiveness factor. The effectiveness factor is correlated against a ratio of two characteristic times, one identified as the time scale of mixing and the other identified as the time scale of reaction. The time scale of mixing is estimated from experimental mixing data, thereby avoiding the use of potentially inaccurate mixing assumptions. In place of reaction experiments, overall reaction rates are generated using a more detailed mixing-cell model. The effectiveness factor correlation is compared against previous models. Because the correlation is based on predicted reaction rates rather than experimentally measured reaction rates, the value of the present work lies in the demonstration of the time scales modeling technique.

INTRODUCTION

In a previous article[1] the authors have shown that several diverse models describing combined reaction and mass transfer in condensation–polymer reactors can be represented by a single formula centered around an effectiveness factor. The form is

$$r_e = \eta r_k \tag{1}$$

where r_k is the reaction rate predicted by kinetics alone, η is the effectiveness factor, and r_e is the overall reaction rate including the effect of mass transfer resistance. They considered models by Ault and Mellichamp[2] and Ravindranath and Mashelkar[3] as well as three original forms. They also developed a general modeling framework based upon a mixing-cell concept and showed that the new framework spans the predictions generated by the previous models.

A major finding from the previous work[1] is that, in every case, the expression for the effectiveness factor can be rearranged to a form that depends on a single dimensionless parameter. Furthermore, the dimensionless parameter can be interpreted as a ratio between a characteristic reaction time and a characteristic mixing time. This is expressed by

$$\eta = f(R) \tag{2}$$

and

$$R = \frac{t_m}{t_r} \tag{3}$$

where t_m is the characteristic mixing time or time scale of mixing and t_r is the characteristic reaction time or time scale of reaction. The form of $f(R)$ changes, depending on the modeling assumptions but shows qualitatively similar behavior in all cases. The form of the time scale of reaction is essentially the same for each model. The form of the time scale of mixing depends on the geometry of the reactor being modeled and choice of assumptions regarding the mixing in the reactor.

The point of departure for the current work is to postulate the existence of an intrinsic and universal form of $f(R)$. It is further postulated that t_m is an inherent property of the process, that t_m depends on

* To whom correspondence should be addressed.

Journal of Applied Polymer Science, Vol. 58, 2095–2100 (1995)
 CCC 0021-8995/95/112095-06

the mixing characteristics only, and that t_m is only crudely estimated when simplifying assumptions are made regarding the geometry and flow behavior. Given this starting point, the challenge is to identify a method to calculate the inherent value of t_m for a given process and subsequently to establish $f(R)$. The potential benefits of this approach are that existing models can be improved once restrictive assumptions are removed and that models for processes with complicated geometry and flows can be developed.

The production of polyethylene terephthalate (PET) in a disc-ring polymer reactor is examined in this article. This is a commercially significant example of this type of process, has received considerable attention from modelers,[2-6] and has a complicated flow pattern that is difficult to model. In order to estimate the time scale of mixing for this system, a scaled-down model of a commercial reactor was constructed using clear plastic and partially filled with an aqueous polyacrylamide solution, which simulates the viscosity of PET at reaction conditions. The flow pattern of a particle embedded in the fluid was observed and used to evaluate the mixing characteristics in the device.

THE TIME SCALE OF MIXING

The experimental mixing apparatus, described in detail elsewhere,[7] contains a single flat circular disc, with a radius of 152 mm, mounted on a horizontal shaft. The shell containing the fluid and the disc is a horizontal cylinder with an inside radius of 175 mm and length of 75 mm. During mixing experiments, the fluid level is maintained about half way to the agitator shaft (75 mm).

When the disc is in motion, a semiregular flow pattern is induced. Fluid elements near the disc follow the disc motion closely, both above and below the surface of the liquid pool. The fluid gradually spirals to the center of the disc where it falls off and enters the liquid pool at some distance from the disc surface. Motion in this area is much slower; however, the fluid eventually approaches the disc surface again and repeats the cycle.

Observation of this flow pattern leads to a conceptual discretization of the flow field into three mixing cells. Figure 1 shows the arrangement of mixing cells along with flows between cells. Flows entering and leaving the system, which would occur in a reactive system but are not part of the mixing experiments, are also shown in Figure 1. Cell 1 is exposed to the vapor and cells 2 and 3 are submerged. Cell 1 is connected by flow to cell 2, and cell 2 is

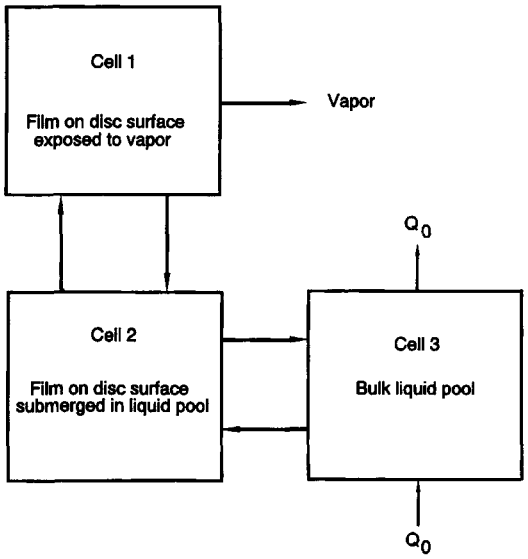

Figure 1 Schematic representation of mixing pattern and mixing cell model.

connected to cell 3, but there is no connection between cell 1 and cell 3. Mixing data generated by experiment consist of records of the cells through which the embedded particle travels and the times when it moves from one cell to another. These data can be used to calculate the flow rates between each pair of cells and the volumes of the cells.[6]

The time scale of mixing is chosen to be the "renewal time" of a fluid element leaving cell 3, traveling to cell 2 and possibly to cell 1 (where evaporation of condensation product occurs) and then again back to cell 3. The choice for the definition of the time scale of mixing is somewhat arbitrary. Similar alternatives were considered but found to yield a worse correlation fit. Furthermore, there is no inherent advantage in this choice of the time scale of mixing definition; the goal of finding a universal model remains for future study.

The renewal time is calculated as follows. The fractions of fluid flow that leave cell 2 and go to either cell 1 or cell 3 are defined based on the flow rates between cells as

$$f_1 = \frac{Q_{21}}{Q_{21} + Q_{23}} \tag{4}$$

and

$$f_3 = \frac{Q_{23}}{Q_{21} + Q_{23}} = 1 - f_1 \tag{5}$$

where f_1 and f_3 are the fractions to cell 1 and cell 3, respectively, and Q_{kj} is the flow from cell k to cell j. Note that the flow pattern assumed in Figure 1

(excluding vapor flow, which is not part of the mixing experiments) forces

$$Q_{12} = Q_{21} \tag{6}$$

and

$$Q_{23} = Q_{32} \tag{7}$$

The average time it takes a fluid element to move from cell i to cell j, given that it eventually goes to cell j, is given by

$$\tau_{ij} = \frac{V_i}{Q_{ij}} \tag{8}$$

The time scale of mixing can be written in terms of the variables defined above as

$$t_m = \tau_{32} + f_3(\tau_{23}) + f_3 f_1(\tau_{21} + \tau_{12} + \tau_{23}) + f_3 f_1^2(2(\tau_{21} + \tau_{12}) + \tau_{23}) + \cdots \tag{9}$$

Equation (9) can be simplified to

$$= \tau_{32} + f_3 \sum_{i=0}^{\infty} f_1^i \tau_{23} + f_3 \sum_{i=0}^{\infty} i f_1^i (\tau_{21} + \tau_{12}) \tag{10}$$

$$= \tau_{32} + \frac{f_3 \tau_{23}}{(1 - f_1)} + \frac{f_1 f_3 (\tau_{21} + \tau_{12})}{(1 - f_1)^2} \tag{11}$$

Defining two new variables, τ_1 and τ_2, as

$$\tau_1 = \tau_{12} + \tau_{21} \tag{12}$$

and

$$\tau_2 = \tau_{32} + \tau_{23} \tag{13}$$

and substituting them into eq. (11) gives

$$t_m = \tau_2 + \frac{f_1}{f_3} \tau_1 \tag{14}$$

The intercell flow rates calculated by the method described above apply to both batch and continuous flow systems. As long as the flow rate from outside the system into any given cell is the same as the flow rate leaving the system from the same cell, and as long as the flow rates into and out of the system are low enough to ignore inertial effects, the intercell flow rates will be unaffected. The vapor flow rate from cell 1 is neglible compared to the intercell flow rates.

THE TIME SCALE OF REACTION

The time scale of reaction has been shown[1] to be independent of the mixing model and given by the form

$$t_r = \frac{K}{4C_B k} \tag{15}$$

where K is the reaction equilibrium constant, k is the forward rate constant and C_B is the concentration of polymer repeat units. The reaction constants correspond to the reversible polycondensation reaction

$$2\mathrm{A} \underset{k/\mathrm{K}}{\overset{k}{\leftrightarrow}} \mathrm{B} + \mathrm{C} \tag{16}$$

where A is the reactive end group, B is the polymer repeat unit, and C is the condensation product. The corresponding rate expression is

$$r_k = k[C_A - 4C_B C_C / K] \tag{17}$$

where C_A and C_C are the concentrations of the polymer end group and the condensation product. By comparing eq. (15) with eq. (17), the time scale of reaction can be interpreted as the inverse of a reaction rate constant for a first-order reaction that consumes the condensation product. This interpretation considers C_B to be a constant.

CORRELATING THE EFFECTIVENESS FACTOR

The form of the correlation for the effectiveness factor given in eq. (2) can be established after estimating t_m, t_r, and r_e for a variety of process conditions. Data sets containing both mixing and reaction results are not available in the literature and were not generated as a part of this work. In place of this, a second model that predicts the overall reaction rate by using a mixing-cell model was used to generate values for r_e for a continuous-flow reactor operating at steady state. The production of polyethylene terephthalate was modeled. Details of this model are given elsewhere.[6,7] Flow rates in the mixing-cell model were based on the same mixing data used to find values of t_m.

Because of the lack of experimental reaction data, the final correlation is essentially a comparison between two models. As such, the importance of the result lies in the demonstration of the use of the

Table I Mixing Experiment Conditions and Results

Exp. No.	Liquid Viscosity (poise)	Liquid Volume (m^3)	Shaft Speed (rpm)	τ_1 (s)	τ_2 (s)	t_m (s)
1	13,000	0.58	0.70	105	4150	4520
2	13,000	0.58	1.1	89	810	1080
3	13,000	0.58	1.4	54	690	860
4	13,000	0.58	2.1	28	290	380
5	13,000	0.65	1.1	67	3090	3690
6	13,000	0.65	1.4	59	740	950
7	13,000	0.65	2.1	39	330	420
8	13,000	0.86	1.1	71	2240	2620
9	13,000	0.86	1.4	65	800	990
10	13,000	0.86	2.1	53	510	630
11	10,500	0.65	4.2	30	260	300

time-scales analysis rather than in the model predictions themselves. When detailed mixing data exists, the mixing-cell model will presumably give more accurate predictions of the overall reaction rate than the effectiveness-factor correlation can. At this point, the successful derivation of an effectiveness-factor correlation represents a single step towards the long term goal of predicting the overall reaction rate based only on the operating variables and kinetic information.

The mixing-cell model is applied to a scaled up analog of the laboratory mixing apparatus, having a 2.8 m inside diameter. The larger size is considered because of its commercial significance. The scale up maintains a constant Reynolds number and Froude number. With these constraints, the rotation rate scales with the disc diameter to the −0.5 power, the flow rate between cells scales with the diameter to the 2.5 power, and the fluid viscosity scales with the diameter to the 1.5 power.

Eleven mixing experiments were conducted in the laboratory scale mixer. The liquid viscosity, liquid level, and rotation rate were varied. Table I contains a summary of the experimental conditions, scaled up to the commercial size, and the time scale of mixing predicted by eq. (14). The mixing experiments could not be completed at lower viscosities because the film adhering to the disc was too thin to entrain the particle embedded in the liquid. The experiments could not be completed at higher viscosities because of difficulties preparing a solution with a high polymer content. The range of liquid volumes corresponds approximately to industrial practice. The range of rotation rates is limited on the low end by the formation of stagnant regions away from the disc and on the high end by a transition to a more turbulent flow pattern. The high rotation rate case may be of industrial interest but could not be studied in this system. This limitation was due to the formation of large numbers of bubbles that obscured the view of the embedded particle.

As expected, the results in Table I indicate that the time scale of mixing and its components τ_1 and τ_2 increase as the liquid volume increases, decrease as the shaft speed increases, and increase as the viscosity increases. The reciprocal of τ_1 would be identical to the shaft speed for fluid elements adhering to a fixed position on the disc. Using values of τ_1 to calculate equivalent shaft speeds gives values that range between 50% and 100% of the corresponding measured shaft speed. Values less than 100% are expected given the shear field existing near the submerged face of the disc (cell 2). A quantitative evaluation of τ_2 is not expected.

Six reaction rates were predicted for each mixing experiment by using the mixing-cell model. The six conditions range over four values of k, corresponding to different temperatures or catalyst concentrations, and three values of the liquid residence time, τ. The liquid residence time is defined as the liquid volume divided by the volumetric feed rate, Q_0. In every case the model considered a prepolymer feed with a degree of polymerization of 50. The rate constant, k, was varied from 10^{-4} m^3/kmol/s to 10^{-1} m^3/kmol/s. This compares to range of $9.17 \cdot 10^{-5}$ m^3/kmol/s to 0.152 m^3/kmol/s reported by Stevenson and Nettleson[8] for polycondensation of PET. Other reaction and physical property parameters correspond to a typical PET manufacturing process. These include an equilibrium constant (K) of 0.5 compared to a range of 0.5 to 1 used by Ravindranath and Mashelkar,[9] an operating pressure of 0.0656 kN/m^2 (0.5 Torr) compared to a range of 0.0656 kN/m^2 to 0.137 kN/m^2 described by Ravindranath and Mashelkar,[10] a temperature of 553K (280°C), and a diffusivity of the condensation product of $1.6 \cdot 10^{-8}$

Table II Mixing-Cell Model Results, τ = 2.5 h

	Effectiveness Factor, η			
Exp. No.	$k = 10^{-1}m^3/kmol/s$	$k = 10^{-2}m^3/kmol/s$	$k = 10^{-3}m^3/kmol/s$	$k = 10^{-4}m^3/kmol/s$
1	0.0024	0.015	0.045	0.081
2	0.011	0.070	0.18	0.32
3	0.014	0.072	0.16	0.31
4	0.029	0.12	0.23	0.47
5	0.0037	0.027	0.093	0.17
6	0.013	0.070	0.16	0.31
7	0.024	0.092	0.18	0.42
8	0.0048	0.030	0.083	0.17
9	0.015	0.057	0.13	0.27
10	0.016	0.059	0.12	0.31
11	0.026	0.073	0.15	0.41

m^2/s compared to a range of $8.2 \cdot 10^{-9}$ m^2/s reported by Rafler et al.[11] to $1.6 \cdot 10^{-8}$ m^2/s reported by Pell and Davis.[12] The vapor pressure of ethylene glycol is calculated using a correlation given by Fontana.[13] Given the values of k, K, and the degree of polymerization in the feed, the time scale of reaction can be calculated from eq. (15). For values of k varying from 10^{-4} $m^3/kmol/s$ to 10^{-1} $m^3/kmol/s$, values of t_r vary from 190 to 0.19 s.

Mixing-cell model results are given in Table II, showing variations with the rate constants, and Table III, showing variations with residence time. Values of R have been calculated from t_m and t_r for each entry in Tables II and III and plotted in Figure 2 along with the effectiveness factor. Two asymptotic conditions are expected for the effectiveness-factor correlation, namely that η should approach 1 as R approaches 0 and that η should approach 0 as R approaches infinity. The choice of axes in Figure 2 allows a straight line with a positive slope to satisfy both asymptotic conditions. The data plotted in Figure 2 show a marked upward curve, which is accommodated by the use of two straight line segments in the fit. The slope of the line segment on the right has been constrained to a value of 1 because results in the first of this series of articles[1] indicate that four of five models investigated show an asymptotic slope of 1 at high values of R. A least squares fit to the data in Figure 2 produces the following three parameter model:

$$\eta = \frac{1}{1 + 1.22R^{0.41}} \quad \text{at} \quad R \leq 1460 \qquad (18)$$

and

$$\eta = \frac{1}{1 + 0.0166R} \quad \text{at} \quad R \geq 1460 \qquad (19)$$

Table III Mixing-Cell Model Results, $k = 10^{-1}m^3/kmol/s$

	Effectiveness Factor, η		
Exp. No.	τ = 0.5 h	τ = 2.5 h	τ = 12.5 h
1	0.0021	0.0024	0.0026
2	0.0098	0.011	0.011
3	0.012	0.014	0.015
4	0.027	0.029	0.030
5	0.0031	0.0037	0.0043
6	0.011	0.013	0.014
7	0.022	0.024	0.025
8	0.0043	0.0048	0.0052
9	0.011	0.012	0.012
10	0.015	0.016	0.016
11	0.023	0.024	0.026

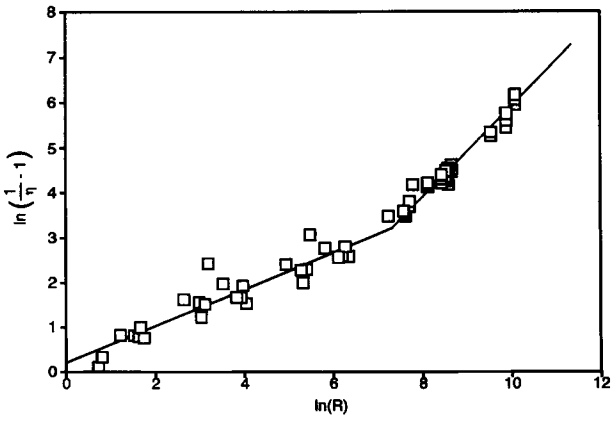

Figure 2 Regression results for the effectiveness factor based on a time-scales analysis.

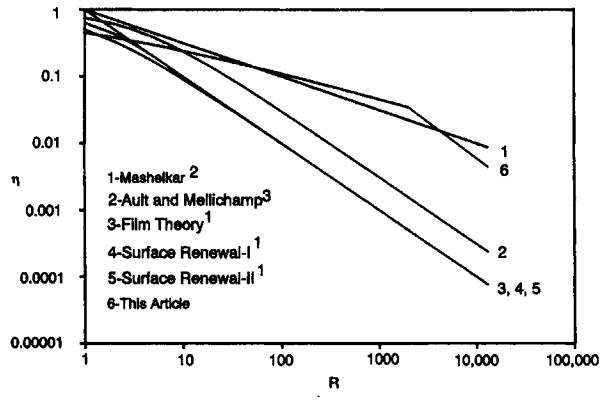

Figure 3 Comparison between current and previous effectiveness-factor correlations.

A comparison between eqs. (18) and (19) and the previous models is presented in Figure 3. The new correlation falls generally within the range of the others.

CONCLUSION

Equations (18) and (19) are important because they have been developed directly from a study of the mixing characteristics of the reaction system, thus demonstrating the feasibility of this approach. They also improve upon previous models because they are free from the effects of any unsupported assumptions regarding the mixing process. The demonstration of this technique is only partial, however, because it is not correlated against experimental, reaction-rate data.

It should also be noted that some elements from the list of overall goals remain for future consideration. An inherent or best definition for the time scale of mixing has not been identified. The definition used here is reasonable and leads to a strong correlation but is somewhat arbitrary. This also implies that the correlation for the effectiveness factor is not universal in any sense.

This material is based upon work supported by the National Science Foundation under Grant CBT-8808709. The U.S. Government has certain rights in this material. The authors express their appreciation for this support.

NOMENCLATURE

A	reactive end group
B	polymer repeat unit
C	condensation product
C_i	concentration of species i (kmol/m^3)
$f(R)$	function of R
f_i	fraction of fluid flow from cell 2 to cell i
k	polycondensation reaction rate constant (m^3/kmol/s)
K	polycondensation reaction equilibrium constant
Q_0	liquid flow rate to and from reactor (m^3/h)
Q_{jk}	volumetric flow rate from cell j to cell k (m^3/s)
R	ratio of the time scale of mixing to the time scale of reaction
r_e	overall reaction rate (kmol/m^3/s)
r_k	kinetic reaction rate (kmol/m^3/s)
t_m	time scale of mixing (s)
t_r	time scale of reaction (s)
V_j	volume of mixing cell j (m^3)
η	effectiveness factor
τ_{ij}	average time a fluid element takes to move from cell i to cell j, given that it eventually moves there (s)
τ	residence time (h)

REFERENCES

1. K. J. Sampson, S. Neogi, and J. C. Medlin, *J. Appl. Polym. Sci.*, **47**, 1040 (1993).
2. K. Ravindranath and R. A. Mashelkar, *Polym. Eng. Sci.*, **22**, 628 (1982).
3. J. W. Ault and D. A. Mellichamp, *Chem. Eng. Sci.*, **27**, 2233 (1972b).
4. C. Laubriet, B. LeCorre, and K. Y. Choi, *Ind. Eng. Chem. Res.*, **30**, 2 (1991).
5. H. C. Saint Martin and K. Y. Choi, *Ind. Eng. Chem. Res.*, **30**, 1712 (1991).
6. S. Neogi and K. J. Sampson, *J. Appl. Polym. Sci.*, to appear.
7. S. Neogi, Ph.D. Dissertation, Ohio University, 1993.
8. R. W. Stevenson and H. R. Nettleson, *J. Polym. Sci.*, **6**, 889 (1968).
9. K. Ravindranath and R. A. Mashelkar, *Developments in Plastic Technology-2*, Elsevier, London, 1985, p. 43.
10. K. Ravindranath and R. A. Mashelkar, *Chem. Eng. Sci.*, **41**, 2197 (1986).
11. G. Rafler, E. Bonatz, G. Reinisch, H. Gajewski, and K. Zacharias, *Acta Polym.*, **30**, 253 (1979).
12. T. M. Pell and T. G. Davis, *J. Polym. Sci.*, **11**, 1671 (1973).
13. C. M. Fontana, *J. Polym. Sci.*, **6**, 2343 (1968).

Received February 23, 1995
Accepted July 2, 1995